MULTI-STAGE GAIN OF THE MICROBUNCHING INSTABILITY*

R. A. Bosch[#] and K. J. Kleman, Synchrotron Radiation Center, University of Wisconsin-Madison,
3731 Schneider Dr., Stoughton, WI 53589, USA
J. Wu, Stanford Linear Accelerator Center, Stanford University, Stanford, CA 94309 USA

Abstract

Bunch compression for a free-electron laser (FEL) may cause growth of current and energy fluctuations at wavelengths shorter than the bunch length. This microbunching instability may disrupt FEL performance or it may be used to produce coherent radiation. We give analytic formulas that approximate microbunching growth and apply them to the Wisconsin FEL (WiFEL).

INTRODUCTION

When a high-current bunch experiences longitudinal impedance before compression in a chicane(s), short-wavelength fluctuations in the current and energy may be amplified [1–8]. This microbunching may render the bunch unsuitable for an FEL [4–7], or it may be used to produce coherent VUV and X-ray radiation [8].

When a bunch's longitudinal distribution is frozen outside of the chicanes, a multi-stage compression and acceleration system may be approximated by staged compression [2, 3, 7–10]. In each stage, a longitudinally-frozen bunch is first affected by longitudinal impedance while it is accelerated. Then it is linearly compressed in a chicane whose impedance is neglected. The model may be refined by representing the impedances within a chicane by effective impedances upstream and downstream of the chicane [7]. At wavelengths shorter than the bunch length, the impedance is typically dominated by longitudinal space charge (LSC) [2–10].

SINGLE-STAGE GAIN

Consider a single stage in which a longitudinally-frozen bunch experiences the longitudinal impedance $Z_{zero}(k_0)$ while being accelerated from energy E_0 to energy E_1. At energy E_1, a chicane under compresses by a factor of $C_1 > 0$, where $R_{56}^{(1)} \leq 0$ is the chicane's energy-to-position matrix element in the convention where it is negative. Large microbunching gain occurs when an initial current modulation passes through the impedance Z_{zero}, generating an energy modulation at the chicane entrance that is converted to a larger current modulation by the chicane's R_{56}. For large microbunching gain of a bunch with initial Gaussian slice energy spread of σ_E, the growth of an initial current modulation with wavenumber k_0 is [2–4, 8]

$$\left| \Delta I / I_{out} / \Delta I / I_{in} \right| = \left| C_1 k_0 R_{56}^{(1)} e Z_{zero}(k_0) I_0 \Big/ E_1 \right| \times \exp\left[-\left(C_1 k_0 R_{56}^{(1)} \sigma_E / E_1 \right)^2 / 2 \right], \quad (1)$$

where $e > 0$ is the magnitude of the electron charge and I_0 is the magnitude of the initial bunch current.

Since the large-gain formula is inapplicable when $R_{56}^{(1)} = 0$ or $Z_{zero}(k_0) = 0$, eq. (1) does note apply for a stage with low growth. For a more general formula, consider a gain matrix S that describes output current and energy modulations due to an input current or energy modulation:

$$S \equiv \begin{pmatrix} S_{II} & S_{IE} \\ S_{EI} & S_{EE} \end{pmatrix}, \quad (2)$$

in which $S_{II} = (\Delta I/I)_{out}/(\Delta I/I)_{in}$, $S_{IE} = (\Delta I/I)_{out}/(\Delta E/E)_{in}$, $S_{EI} = (\Delta E/E)_{out}/(\Delta I/I)_{in}$, and $S_{EE} = (\Delta E/E)_{out}/(\Delta E/E)_{in}$.

The matrix elements of S, which describe a stage consisting of acceleration followed by compression, may be obtained from a similar matrix T that describes compression followed by acceleration [7, 9–10]. To do so, we consider the special cases of acceleration without compression and compression without acceleration.

For a bunch that is accelerated from energy E_0 to energy E_1 while experiencing impedance $Z_{zero}(k_0)$ [7, 9]

$$T_{II} = 1, \quad (3a)$$

$$T_{IE} = 0, \quad (3b)$$

$$T_{EI} = -eZ_{zero}(k_0)I_0 / E_1, \quad (3c)$$

$$T_{EE} = E_0 / E_1. \quad (3d)$$

For compression by a factor of C_1 at energy E_1 in a chicane with energy-to-position matrix element $R_{56}^{(1)}$ [7, 9]

$$T_{II} = F^{(1)}, \quad (4a)$$

$$T_{IE} = iF^{(1)}C_1 k_0 R_{56}^{(1)}, \quad (4b)$$

$$T_{EI} = iG^{(1)}C_1 / E_1, \quad (4c)$$

$$T_{EE} = F^{(1)}C_1 - G^{(1)}C_1^2 k_0 R_{56}^{(1)} / E_1. \quad (4d)$$

The reduction in growth at short wavelengths caused by the bunch's energy spread is described by

$$F^{(1)} = \int \cos(k_0 C_1 R_{56}^{(1)} \delta / E_1) f(\delta) d\delta, \quad (5a)$$

$$G^{(1)} = \int \delta \sin(k_0 C_1 R_{56}^{(1)} \delta / E_1) f(\delta) d\delta. \quad (5b)$$

Here, δ is the energy deviation of an electron and $f(\delta)$ is the normalized energy distribution of each slice of the uncompressed bunch.

If the T matrix for acceleration is multiplied on the left by the T matrix for compression, we obtain the matrix S

$$S_{II} = F^{(1)} - iF^{(1)}C_1 k_0 R_{56}^{(1)} e Z_{zero}(k_0) I_0 / E_1, \qquad (6a)$$

$$S_{IE} = iF^{(1)}C_1 k_0 R_{56}^{(1)} E_0 / E_1, \qquad (6b)$$

$$S_{EI} = -F^{(1)}C_1 e Z_{zero}(k_0) I_0 / E_1 + iG^{(1)}C_1 / E_1$$
$$+ G^{(1)}C_1^2 k_0 R_{56}^{(1)} e Z_{zero}(k_0) I_0 / E_1^2 \qquad (6c)$$

$$S_{EE} = F^{(1)}C_1 E_0 / E_1 - G^{(1)}C_1^2 k_0 R_{56}^{(1)} E_0 / E_1^2. \qquad (6d)$$

Equation (1) corresponds to the approximation in which only the second term on the RHS of eq. (6a) is retained.

MULTI-STAGE GAIN

Consider several stages that consist of acceleration followed by compression. In the first stage, a longitudinally-frozen chirped bunch with energy E_0 and peak current magnitude I_0 passes through impedance Z_{zero} while being accelerated to energy E_1. It is then compressed by a factor of C_1 by the energy-to-position matrix element $R_{56}^{(1)}$ of the first chicane.

In the second stage, the frozen bunch passes through impedance Z_1 while being accelerated from energy E_1 to energy E_2. It is then compressed by a factor of C_2 by the $R_{56}^{(2)}$ of the second chicane. In the n-th stage, the frozen bunch passes through impedance Z_{n-1} while being accelerated from energy E_{n-1} to energy E_n. The chirped bunch is then compressed by a factor C_n by the matrix element $R_{56}^{(n)}$ of the n-th chicane.

For two stages, the gain matrix S may be obtained by modeling the rotated phase space entering the second stage [7]. For more than two stages, such expressions become intractable. However, if we neglect the phase-space rotation at the entrance of the n-th stage for $n > 1$, multistage gain may be approximated by matrix multiplication of the single-stage gain matrix, as in the case of a cold bunch. The gain matrix for N stages is $S \approx S^{(N)}S^{(N-1)} \dots S^{(1)}$ [9], where the matrix $S^{(n)}$ for the n-th stage is given by eq. (6), in which the compression factor, R_{56}, impedance and energies describe the n-th stage, while the wavenumber, current and energy distribution describe the entrance of the n-th stage. The elements of $S^{(n)}$ are

$$S_{II}^{(n)} = F^{(n)}$$
$$- iF^{(n)}(\textstyle\prod_{j=1}^{n-1}C_j^2)C_n k_0 R_{56}^{(n)} e Z_{n-1}[(\textstyle\prod_{j=1}^{n-1}C_j)k_0]I_0 / E_n, \qquad (7a)$$

$$S_{IE}^{(n)} = iF^{(n)}(\textstyle\prod_{j=1}^{n}C_j)k_0 R_{56}^{(n)} E_{n-1} / E_n, \qquad (7b)$$

$$S_{EI}^{(n)} = -F^{(n)}(\textstyle\prod_{j=1}^{n}C_j)e Z_{n-1}[(\textstyle\prod_{j=1}^{n-1}C_j)k_0]I_0 / E_n$$
$$+ iG^{(n)}C_n / E_n \qquad (7c)$$
$$+ G^{(n)}(\textstyle\prod_{j=1}^{n}C_j^2)k_0 R_{56}^{(n)} e Z_{n-1}[(\textstyle\prod_{j=1}^{n-1}C_j)k_0]I_0 / E_n^2,$$

$$S_{EE}^{(n)} = \frac{F^{(n)}C_n E_{n-1}}{E_n} - \frac{G^{(n)}(\prod_{j=1}^{n}C_j)C_n k_0 R_{56}^{(n)} E_{n-1}}{E_n^2}. \qquad (7d)$$

where

$$F^{(n)} = \int \cos[(\textstyle\prod_{j=1}^{n-1}C_j^2)C_n k_0 R_{56}^{(n)}\delta / E_n]f(\delta)d\delta, \qquad (8a)$$

$$G^{(n)} = (\textstyle\prod_{j=1}^{n-1}C_j)\int \delta\sin[(\textstyle\prod_{j=1}^{n-1}C_j^2)C_n k_0 R_{56}^{(n)}\delta / E_n]f(\delta)d\delta. \qquad (8b)$$

Here, $f(\delta)$ is the energy distribution of each slice of the uncompressed bunch, while k_0 is the wavenumber of the initial modulation in the uncompressed bunch.

For a Gaussian energy distribution with initial rms energy spread of σ_E, eq. (8) gives [7]

$$F^{(n)} = \exp\{-[(\textstyle\prod_{j=1}^{n-1}C_j^2)C_n k_0 R_{56}^{(n)}\sigma_E / E_n]^2 / 2\}, \qquad (9a)$$

$$G^{(n)} = [(\textstyle\prod_{j=1}^{n-1}C_j^3)C_n k_0 R_{56}^{(n)}\sigma_E^2 / E_n]$$
$$\times \exp\{-[(\textstyle\prod_{j=1}^{n-1}C_j^2)C_n k_0 R_{56}^{(n)}\sigma_E / E_n]^2 / 2\}, \qquad (9b)$$

When the uncompressed bunch has an rms energy spread σ_E from heating by a matched laser heater, the energy distribution may be approximated by a semicircular distribution [4], in which case [7]

$$F^{(n)} = [(\textstyle\prod_{j=1}^{n-1}C_j^2)C_n k_0 R_{56}^{(n)}\sigma_E / E_n]^{-1}$$
$$\times J_1[2(\textstyle\prod_{j=1}^{n-1}C_j^2)C_n k_0 R_{56}^{(n)}\sigma_E / E_n], \qquad (10a)$$

$$G^{(n)} = [(\textstyle\prod_{j=1}^{n}C_j)k_0 R_{56}^{(n)} / 2E_n]^{-1}$$
$$\times J_2[2(\textstyle\prod_{j=1}^{n-1}C_j^2)C_n k_0 R_{56}^{(n)}\sigma_E / E_n], \qquad (10b)$$

Note that $F^{(3)}$, $G^{(2)}$ and $G^{(3)}$ differ from the quantities F_3, G_2 and G_3 that are defined in Ref. [7].

Calculating the microbunching gain using S matrices to describe stages consisting of acceleration followed by compression is equivalent to using T matrices to describe stages consisting of compression followed by acceleration. Thus, the approximate agreement between the WiFEL microbunching gain in T-matrix calculations and tracking simulations [7, 9, 10] confirms the approximate validity of S-matrix calculations.

SHOT NOISE

Typically, microbunching at short wavelengths is driven by the impedance of longitudinal space charge (LSC), and the LSC impedances within the chicanes may be neglected due to longitudinal smearing [3, 7, 8]. To test the validity of this approximation for WiFEL, we consider the single-stage and two-stage compression schemes shown in Figure 1, for a 200-pC bunch with an initial Gaussian energy spread of 3 keV. For both schemes, the microbunching gain calculated by matrix multiplication is in good agreement with tracking simulations [7, 9, 10].

To avoid seeding the microbunching instability, the WiFEL electron gun operates in the blow-out mode to provide frozen bunches with a smooth longitudinal profile [11]. However, a 200-pC bunch has a finite number of electrons ($N_b = 1.25 \times 10^9$) whose positions vary from shot to shot. The initial shot noise at wavelength λ_0 is characterized by rms current and energy modulations at 4 MeV that obey [5, 8–10, 12]

$$\begin{pmatrix} \Delta I / I_{\mathrm{in}}(\lambda_0) \\ \Delta E / E_{\mathrm{in}}(\lambda_0) \end{pmatrix} = \begin{pmatrix} 1/\sqrt{N_b} \\ 0 \end{pmatrix}. \quad (11)$$

For bunches with a fixed number of independent particles, eq. (11) applies for short wavelengths where the longitudinal profile's form factor is negligible [12]. For bunches that are produced by a Poisson process, eq. (11) gives the rms shot noise for all wavelengths [12].

For single-stage compression followed by acceleration to 1.7 GeV, we calculate the microbunching gain by multiplying two S matrixes. The matrix $S^{(1)}$ describes acceleration from 4 MeV to 400 MeV, followed by factor-of-20 compression in a chicane with $R_{56}^{(1)} = -100$ mm. The matrix $S^{(2)}$ describes acceleration from 400 MeV to 1.7 GeV, followed by factor-of-one compression in a dummy chicane with $R_{56}^{(2)} = 0$. Multiplying eq. (11) by $S^{(2)}S^{(1)}$ predicts the rms current and energy fluctuations at 1.7 GeV from linear growth of the shot noise.

In Figure 2(a), red curves show the calculated microbunching caused by the impedances of LSC, coherent synchrotron radiation in bending magnets (CSR), coherent edge radiation downstream of bending magnets (CER), and geometric linac wakes. Impedance within the chicane is represented by effective impedances before and after the chicane [7]. The LSC impedances are calculated for a round beam with effective radius $r_b = 0.85(\sigma_x + \sigma_y)$ [4], in which σ_x and σ_y are beam dimensions for normalized transverse emittance of 1 μm-rad and $\langle\beta_x\rangle = \langle\beta_y\rangle = 25$ m. Blue curves show the calculated microbunching from the LSC impedance outside of the chicane. The agreement between the red and blue curves confirms that nearly all of the microbunching is due to
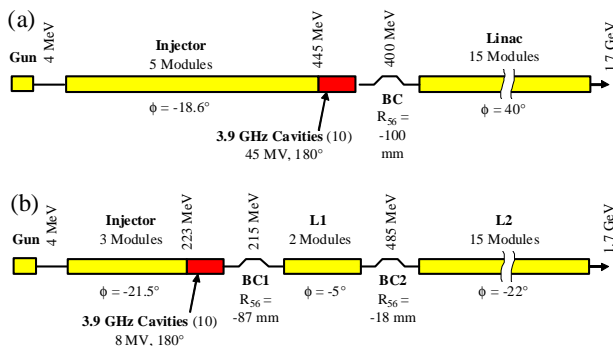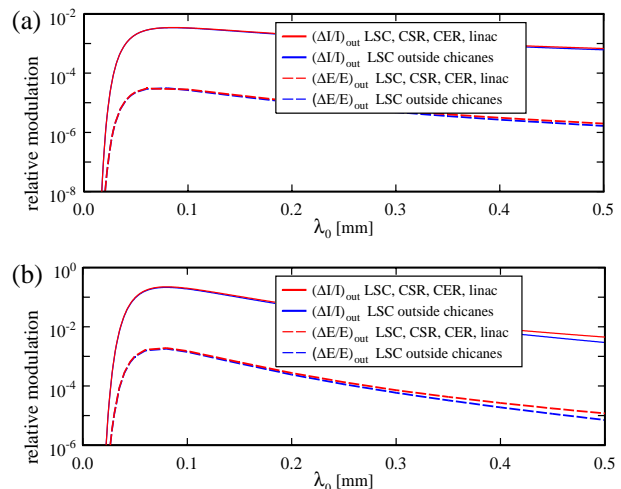
Figure 2: Microbunching after compression and acceleration to 1.7 GeV. (a) Single-stage compressor. (b) Two-stage compressor.

LSC impedance outside of the chicanes.

Figure 2(b) displays similar calculations for two-stage compression followed by acceleration to 1.7 GeV, performed by multiplying three S matrices. The first matrix describes acceleration from 4 MeV to 215 MeV followed by a factor-of-eight compression in a chicane with $R_{56}^{(1)} = -87$ mm. The second matrix describes acceleration from 215 MeV to 485 MeV followed by factor-of-2.5 compression in a chicane with $R_{56}^{(2)} = -18$ mm. The third matrix describes acceleration from 485 MeV to 1.7 GeV, followed by a factor-of-one compression in a dummy chicane with $R_{56}^{(3)} = 0$. Multiplying eq. (11) by $S^{(3)}S^{(2)}S^{(1)}$ predicts the rms current and energy fluctuations at 1.7 GeV from linear growth of the shot noise. Again, nearly all of the microbunching is due to LSC impedance outside of the chicanes.

The output current modulations of Fig. 2 are consistent with using eq. (1) to describe each stage of compression, which is consistent with stages that have high gain. Note that eq. (1) cannot be used for the subsequent stage that has a dummy chicane with $R_{56} = 0$.

After acceleration to 1.7 GeV, the WiFEL bunches are distributed to the FELs by a beam spreader consisting of a three-stage binary separation tree and collimator [9, 10]. Tracking simulations have previously verified that the microbunching at the exit of the spreader is approximated by multiplying S matrices (or T matrices) that represent the LSC impedances and R_{56} values of the spreader stages and collimator [9, 10]. Figure 3 shows the calculated microbunching from shot noise at the exit of the beam spreader for our original spreader design that has a total R_{56} value of 950 μm.

Figure 3 also shows the current modulations calculated by using eq. (1) to describe each chicane and non-dummy spreader stage. Equation (1) does not accurately predict the gain of the spreader stages, whose R_{56} values are much smaller than the bunch-compressor chicanes.

Figure 1: Schematic diagrams for two bunch compressors. (a) Single-stage compressor. (b) Two-stage compressor.
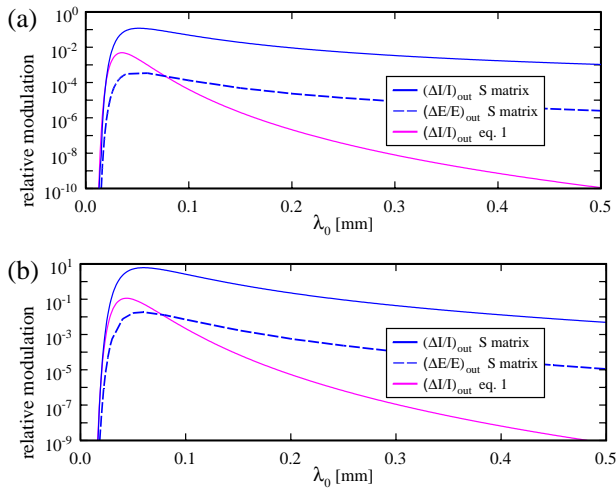
Figure 3: Microbunching after compression, acceleration to 1.7 GeV, and passage through the original beam spreader design that has $R_{56} = 950$ μm. (a) Single-stage compressor. (b) Two-stage compressor.

Figure 4 displays microbunching calculations for a modified beam spreader design that is nearly isochronous ($R_{56} = 0$). Using the isochronous spreader reduces the microbunching gain by an order of magnitude. Again, eq. (1) does not accurately model the spreader stages.

If single-stage compression is used with an isochronous beam spreader, Fig. 4 predicts that the microbunching from shot noise satisfies the WiFEL requirement that the relative current and energy modulations be smaller than 10% and 3×10^{-4} at all wavelengths. This is confirmed by tracking simulations that approximate shot-noise-induced microbunching [10].

SUMMARY

We have provided analytic formulas for the microbunching gain of an FEL driver that can be modeled
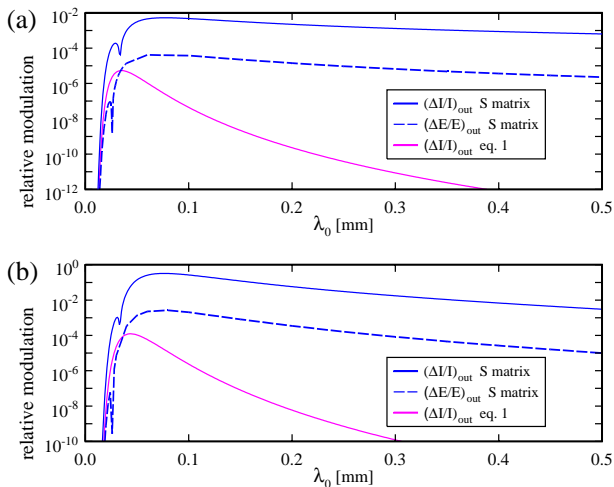
Figure 4: Microbunching after compression, acceleration to 1.7 GeV, and passage through an isochronous beam spreader. (a) Single-stage compressor. (b) Two-stage compressor.

as staged compression. For the n-th stage, in which a longitudinally frozen bunch passes through a longitudinal impedance before compression in a chicane, a matrix $S^{(n)}$ describes growth of current and energy modulations. The gain matrix for N stages is $S \approx S^{(N)} S^{(N-1)} \dots S^{(1)}$.

For WiFEL one-stage and two-stage compression schemes, previous tracking simulations have confirmed the approximate validity of the analytic gain calculation when the impedances of LSC, CSR, CER, and the linac geometry are all included. In this article, we showed that nearly all of the WiFEL microbunching growth is due to the LSC impedance outside of the chicanes.

For a typical case where the LSC impedance causes microbunching, the formulas may be used to estimate the microbunching growth without detailed impedance modeling of CSR, CER and the linac geometry. Stages with small microbunching gain may be included. In the S matrix calculation, the growth of current modulations and energy modulations are both predicted.

REFERENCES

[1] M. Borland, Y.-C. Chae, S. Milton, R. Soliday, V. Bharadwaj, P. Emma, P. Krejcik, C. Limborg, H.-D. Nuhn and M. Woodley, in "Proceedings of the 2001 Particle Accelerator Conference, Chicago" (IEEE, Piscataway, NJ, 2001), p. 2707.

[2] E. L. Saldin, E. A. Schneidmiller and M. V. Yurkov, Nucl. Instrum. Methods Phys. Res., Sect. A 483, 516 (2002).

[3] E. L. Saldin, E. A. Schneidmiller and M. V. Yurkov, Nucl. Instrum. Methods Phys. Res., Sect. A 528, 355 (2004).

[4] Z. Huang, M. Borland, P. Emma, J. Wu, C. Limborg, G. Stupakov and J. Welch, Phys. Rev. ST Accel. Beams 7, 074401 (2004).

[5] M. Venturini, Phys. Rev. ST Accel. Beams 10, 104401 (2007).

[6] M. Venturini and A. Zholents, Nucl. Instrum. Methods Phys. Res., Sect. A 593, 53 (2008).

[7] R. A. Bosch, K. J. Kleman and J. Wu, Phys. Rev. ST Accel. Beams 11, 090702 (2008).

[8] E. A. Schneidmiller and M. V. Yurkov, DESY 10-048, 2010.

[9] R. A. Bosch, K. J. Kleman and J. Wu, in "Proceedings of the 2009 Particle Accelerator Conference, Vancouver, Canada" (IEEE, Piscataway, NJ, 2010), WE5RFP057.

[10] R. A. Bosch, K. J. Kleman and J. Wu, in "Proceedings of the 2009 Particle Accelerator Conference, Vancouver, Canada" (IEEE, Piscataway, NJ, 2010), WE5RFP058.

[11] R. Legg, W. Graves, T. Grimm and P. Piot, in "Proceedings of the 11th European Particle Accelerator Conference, Genoa, Italy, 2008" (EPS-AG, Genoa, Italy, 2008), p. 469.

[12] R. A. Bosch and R. J. Bosch, in "Proceedings of the 31st International Free Electron Laser Conference (FEL 09), Liverpool, UK" (STFC Daresbury Laboratory, Warrington, 2009), p. 123.